

10-27-2022

Transcriptional Profiles in Olfactory Pathway-Associated Brain Regions of African Green Monkeys: Associations With Age and Alzheimer's Disease Neuropathology


Jacob D Negrey
Wake Forest School of Medicine

Dorothy L Dobbins
Wake Forest School of Medicine

Timothy D Howard
Wake Forest School of Medicine

Karin E Borgmann-Winter
Thomas Jefferson University

Follow this and additional works at: https://jdc.jefferson.edu/department_neuroscience

 Part of the [Neurosciences Commons](#), and the [Psychiatry and Psychology Commons](#)

[Let us know how access to this document benefits you](#)

See next page for additional authors

Recommended Citation

Negrey, Jacob D; Dobbins, Dorothy L; Howard, Timothy D; Borgmann-Winter, Karin E; Hahn, C G; Kalinin, Sergey; Feinstein, Douglas L; Craft, Suzanne; Shively, Carol A; and Register, Thomas C, "Transcriptional Profiles in Olfactory Pathway-Associated Brain Regions of African Green Monkeys: Associations With Age and Alzheimer's Disease Neuropathology" (2022). *Department of Neuroscience Faculty Papers*. Paper 75. https://jdc.jefferson.edu/department_neuroscience/75

This Article is brought to you for free and open access by the Jefferson Digital Commons. The Jefferson Digital Commons is a service of Thomas Jefferson University's [Center for Teaching and Learning \(CTL\)](#). The Commons is a showcase for Jefferson books and journals, peer-reviewed scholarly publications, unique historical collections from the University archives, and teaching tools. The Jefferson Digital Commons allows researchers and interested readers anywhere in the world to learn about and keep up to date with Jefferson scholarship. This article has been accepted for inclusion in Department of Neuroscience Faculty Papers by an authorized administrator of the Jefferson Digital Commons. For more information, please contact: JeffersonDigitalCommons@jefferson.edu.

Authors

Jacob D Negrey, Dorothy L Dobbins, Timothy D Howard, Karin E Borgmann-Winter, C G Hahn, Sergey Kalinin, Douglas L Feinstein, Suzanne Craft, Carol A Shively, and Thomas C Register

RESEARCH ARTICLE

Transcriptional profiles in olfactory pathway-associated brain regions of African green monkeys: Associations with age and Alzheimer's disease neuropathology

Jacob D. Negrey¹ | Dorothy L. Dobbins¹ | Timothy D. Howard² |
Karin E. Borgmann-Winter³ | Chang-Gyu Hahn³ | Sergey Kalinin⁴ |
Douglas L. Feinstein^{4,5} | Suzanne Craft^{6,7} | Carol A. Shively^{1,7} | Thomas C. Register^{1,7}

¹Department of Pathology/Comparative Medicine, Wake Forest School of Medicine, Winston-Salem, North Carolina, USA

²Department of Biochemistry, Wake Forest School of Medicine, Winston-Salem, North Carolina, USA

³Department of Psychiatry, Department of Neuroscience, Thomas Jefferson University, Philadelphia, PA, USA

⁴Department of Anesthesiology, University of Illinois, Chicago, Illinois, USA

⁵Research and Development, Jesse Brown VA Medical Center, Chicago, Illinois, USA

⁶Department of Internal Medicine/Gerontology and Geriatric Medicine, Wake Forest School of Medicine, Winston-Salem, North Carolina, USA

⁷Wake Forest Alzheimer's Disease Research Center, Winston-Salem, North Carolina, USA

Correspondence

Thomas C. Register, Department of Pathology/Comparative Medicine, Wake Forest School of Medicine, Medical Center Blvd, Winston-Salem, NC 27157-1040, USA.
Email: register@wakehealth.edu

Funding information

National Institutes of Health, Grant/Award Numbers: P30AG021332, P30AG049638, P40OD010965, RF1AG058829, R24AG073199; Department of Veterans Affairs, Grant/Award Numbers: VA 247-P-0447, VA 240-12-C-0051; Roena Kulynych Center for Memory and Cognition Research of Wake Forest School of Medicine

Abstract

Introduction: Olfactory impairment in older individuals is associated with an increased risk of Alzheimer's disease (AD). Characterization of age versus neuropathology-associated changes in the brain olfactory pathway may elucidate processes underlying early AD pathogenesis. Here, we report age versus AD neuropathology-associated differential transcription in four brain regions in the olfactory pathway of 10 female African green monkeys (vervet, *Chlorocebus aethiops sabaesus*), a well-described model of early AD-like neuropathology.

Methods: Transcriptional profiles were determined by microarray in the olfactory bulb (OB), piriform cortex (PC), temporal lobe white matter (WM), and inferior temporal cortex (ITC). Amyloid beta (A β) plaque load in parietal and temporal cortex was determined by immunohistochemistry, and concentrations of A β 42, A β 40, and norepinephrine in ITC were determined by enzyme-linked immunosorbent assay (ELISA). Transcriptional profiles were compared between middle-aged and old animals, and associations with AD-relevant neuropathological measures were determined.

Results: Transcriptional profiles varied by brain region and age group. Expression levels of *TRO* and *RNU4-1* were significantly lower in all four regions in the older group. An additional 29 genes were differentially expressed by age in three of four regions.

This is an open access article under the terms of the [Creative Commons Attribution-NonCommercial-NoDerivs](https://creativecommons.org/licenses/by-nc-nd/4.0/) License, which permits use and distribution in any medium, provided the original work is properly cited, the use is non-commercial and no modifications or adaptations are made.

© 2022 The Authors. *Alzheimer's & Dementia: Translational Research & Clinical Interventions* published by Wiley Periodicals LLC on behalf of Alzheimer's Association.

Analyses of a combined expression data set of all four regions identified 77 differentially expressed genes (DEGs) by age group. Among these DEGs, older subjects had elevated levels of *CTSB*, *EBAG9*, *LAMTOR3*, and *MRPL17*, and lower levels of *COMMD10* and *TYW1B*. A subset of these DEGs was associated with neuropathology biomarkers. Notably, *CTSB* was positively correlated with A β plaque counts, A β 42:A β 40 ratios, and norepinephrine levels in all brain regions.

Discussion: These data demonstrate age differences in gene expression in olfaction-associated brain regions. Biological processes exhibiting age-related enrichment included the regulation of cell death, vascular function, mitochondrial function, and proteostasis. A subset of DEGs was specifically associated with AD phenotypes. These may represent promising targets for future mechanistic investigations and perhaps therapeutic intervention.

KEYWORDS

aging, Alzheimer's disease, mRNA, nonhuman primates, olfactory pathway, transcriptomics, vervet

1 | INTRODUCTION

Olfactory impairment co-occurs at high prevalence with Alzheimer's disease (AD) and mild cognitive impairment.¹⁻³ In addition, olfactory function generally declines with age, but impairment is more severe in patients with AD and mild cognitive impairment,⁴ and develops in tandem with AD neuropathology.^{2,5} In mice and humans, olfaction-associated brain regions, especially the olfactory bulb (OB), are among the first brain regions to exhibit AD-associated pathology.^{6,7} Older individuals experiencing olfactory impairment have over three times the risk of developing cognitive impairment⁸ and over twice the risk of developing dementia in the next 5 years.⁹ Combining olfactory memory and odor identification further increases the power for predicting AD development.¹⁰ Altogether, olfactory impairment represents a promising indicator of prodromal AD.¹¹ Characterizing changes that occur in the olfactory pathway during aging and in preclinical AD may help illuminate processes underlying early AD neuropathogenesis.

Specific mechanisms underlying the close associations between olfactory dysfunction and subsequent diagnosis of cognitive impairment have not been identified. Phenotypic hallmarks of AD such as amyloid beta (A β) and phosphorylated tau (p-tau) accumulation have been implicated in AD-associated olfactory dysfunction.² In Tg2576 mice, the OB is among the first brain regions to exhibit A β accumulation, and the degree of olfactory-associated behavioral deficits (e.g., odor investigation) correlates with A β accumulation.⁷ In a longitudinal human cohort, A β and tau burden, particularly in the entorhinal cortex, accounted for more than 10% of variation in odor identification.¹² The apolipoprotein E (*APOE*) ϵ 4 variant has been associated with olfactory dysfunction in both rodent models and humans,^{13,14} and also implicated in olfactory dysfunction in the absence of AD.¹⁵ Finally, the dysregulation of norepinephrine (NE), a catecholamine that con-

tributes to stability and retrieval of olfactory memory,¹⁶ has long been observed in patients with AD.¹⁷ These findings suggest complex relationships between AD and related dementias, and pathophysiological mechanisms in the olfactory system.

Studies of processes contributing to olfactory dysfunction in pre-clinical models are useful in understanding relationships with AD. African green monkeys, or vervets (*Chlorocebus aethiops sabaues*), are a well-described nonhuman primate (NHP) model of aging and early AD-like neuropathology and other AD-relevant phenotypes, including cognition, physical function, and fluid biomarkers.¹⁸⁻²² Although vervets do not exhibit the severity of neuropathological phenotypes observed in human AD, vervet cognitive performance and physical function (e.g., gait speed) decrease with age,¹⁹ and A β plaque load is greater in the brains of old versus middle-aged vervets^{20,22} and correlated negatively with gait speed.²¹ A β 40 and A β 42 levels in cerebrospinal fluid (CSF) decreased with age and were inversely associated with A β 42 levels in temporal cortex.²¹ Although paired helical filament (PHF)-tau in vervet brains rarely presents as neurofibrillary tangles, PHF-tau burden was negatively correlated with bilateral volumes of insula, cerebellum, and left temporal lobe, whereas levels of p-tau181 in CSF was negatively correlated with prefrontal and temporal lobe volumes.²¹ Thus, aged vervet monkeys recapitulate many characteristics of early AD-like neuropathology and may help illuminate processes underlying early AD pathogenesis.

The purpose of the present study was to identify neurobiological processes in olfaction-associated brain regions that vary with age and/or associate with biomarkers of AD neuropathogenesis. Subjects were 10 healthy middle-aged and old female vervets in which we measured messenger RNA (mRNA) transcripts in four brain regions important to the olfactory pathway. First, we assessed transcriptomic differences in brain regions by age and then determined their co-variation with biomarkers of AD, including A β plaque counts in the

posterior temporal lobe, and levels of A β 42 and A β 40 peptides and NE in the inferior temporal cortex (ITC). We suggest that relationships between AD biomarkers and transcript levels in vervet brain may facilitate the identification of genes of interest in the study of early AD pathogenesis in the olfactory pathway.

2 | METHODS

2.1 | Subjects

We studied brain tissue from five middle-aged (median = 11.4, range = 9.3–11.6 years; corresponding roughly to humans 35 years of age), and five old (median = 23.6, range = 19.7–26.2 years, corresponding roughly to humans aged >70 years of age) female vervets. Subjects were from the Vervet Research Colony (VRC) at Wake Forest School of Medicine. Enclosures provided ≈ 28 m² indoors and 111 m² outdoors. Monkeys were fed standard monkey chow, and water was available ad libitum. The brains in this project were available as a part of a multidisciplinary pilot project exploring relationships of age with physiologic and functional phenotypes in healthy middle-aged and old subjects. Details regarding vervet husbandry and housing are available elsewhere.^{19,23–25} All procedures were conducted in accordance with state and federal laws, standards of the Department of Health and Human Services, and guidelines established by the Institutional Animal Care and Use Committee. Details regarding methods for tissue collection and AD phenotypes are presented in the [Supplemental Methods](#).

2.2 | RNA isolation

RNA was isolated from OB, piriform cortex (PC), ITC, and white matter (WM) using the AllPrep DNA/RNA Mini Kit (Qiagen, Inc., Hilden, Germany). RNA quantity was determined using a NanoDrop spectrophotometer, and quality by integrity of 18s and 28s ribosomal RNA using the Agilent 2100 Bioanalyzer with RNA 6000 Nano chips (Agilent Technology, Inc., Santa Clara, CA, USA) following the manufacturer's instructions. RNA samples with RIN (RNA integrity) scores >7.0 were used for expression microarrays.

2.3 | Microarrays

Illumina HumanHT-12 v4 Expression BeadChip Arrays were used to perform genome-wide expression analyses. The Illumina TotalPrep-96 RNA Amplification Kit (Ambion/Applied Biosystems, Darmstadt, Germany) was used for reverse transcription, and amplification with 50 to 500 ng of input total RNA (at 11 μ L). All samples from a specific region were assessed on a single BeadChip, and a stratified approach was used to assign the individual samples to specific (12 samples/chip) positions on the chip. Arrays were read using the Illumina HiScan system. Data pre-processing, which included correction for local background

RESEARCH IN CONTEXT

- 1. Systematic review:** We performed a targeted literature review using online search features. We cite several recent reviews describing current knowledge and remaining questions concerning the olfactory system in aging and early Alzheimer's disease (AD) pathogenesis. Although associations between olfactory deficits, aging, and AD pathology are well documented, the exact mechanisms leading to AD-related olfactory dysfunction are not yet fully understood.
- 2. Interpretation:** Our hypothesis-generating research suggests genes and regulatory networks associated with aging in olfaction-associated brain regions in vervets. Our work also pinpoints a subset of genes uniquely associated with AD-relevant phenotypes.
- 3. Future directions:** Our results highlight promising gene targets for mechanistic studies of AD pathogenesis. Our research also suggests biological pathways strongly associated with AD neuropathology, including vascular function, mitochondrial function, and proteostasis. Finally, these results underscore the vervet's utility as a model for early AD-like neuropathology.

and quality control (QC) analyses, were performed using Illumina's GenomeStudio.

2.4 | Bioinformatics

We conducted differential gene expression (DGE) analyses using the *limma* package v3.48.3²⁶ in R v4.1.1.²⁷ We performed two sets of analyses: one in which we analyzed expression data across all brain regions with adjustment for multiple sampling of individuals, and a second in which we analyzed each brain region independently. When analyzing all four brain regions together, we considered genes "differentially expressed" if they had a Benjamini-Hochberg false discovery rate (FDR) <0.05. When analyzing each brain region independently, we considered DEGs to be those with an unadjusted *p*-value <0.05 and a |fold change value| >1.2, as sample sizes for individual regions were relatively small, and power was therefore low. We do not report differentially expressed probes that were unannotated. Additional information regarding DGE analyses are provided in the [Supplementary Methods](#).

2.5 | Ingenuity Pathway Analysis

DEG sets were evaluated using Ingenuity Pathway Analysis (IPA; Qiagen, Hilden, Germany) to identify associated processes and regulatory networks. We performed separate analyses for DEGs identified in

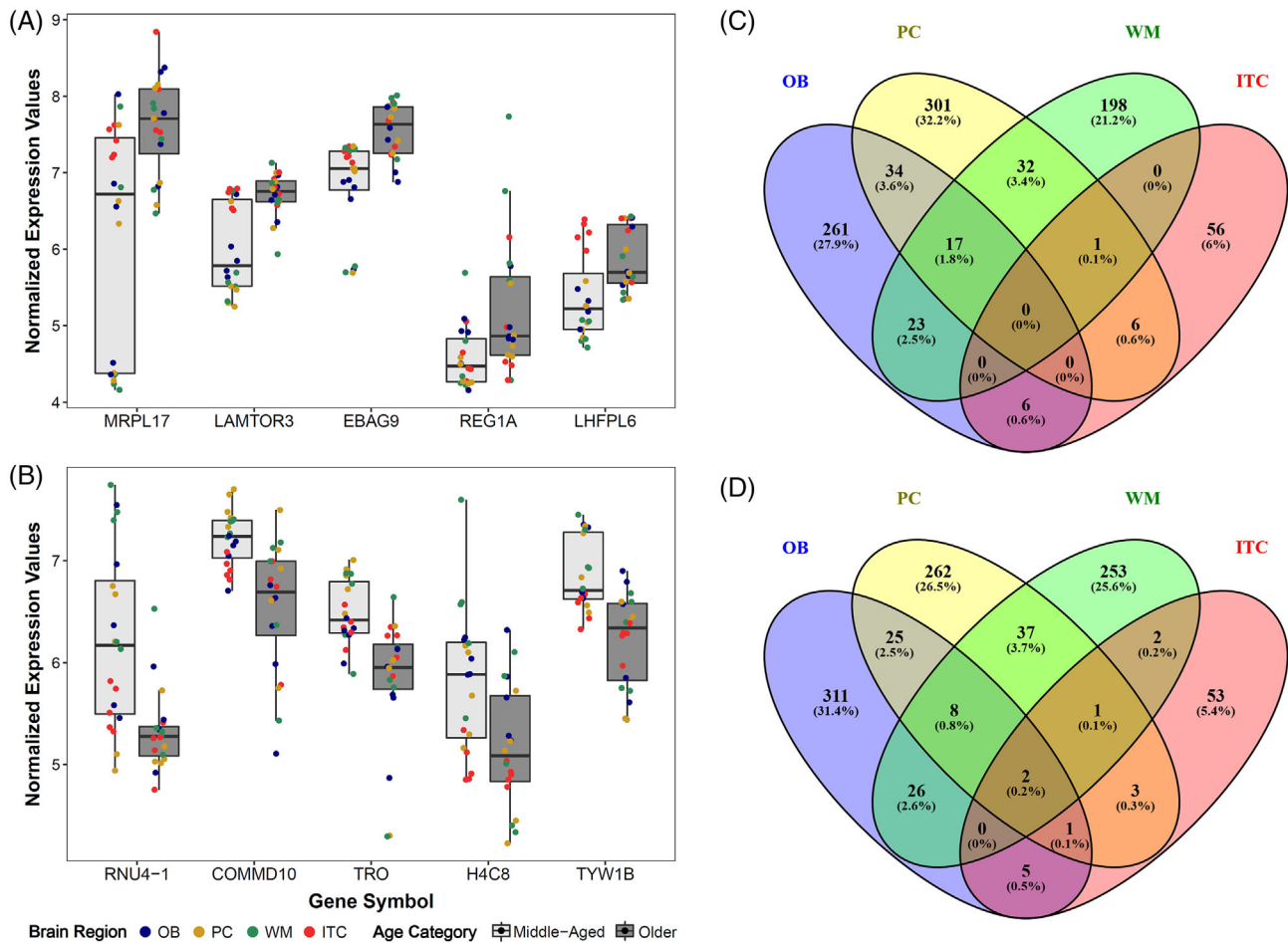


FIGURE 1 Regional variation in differentially expressed genes (DEGs) by age. Boxplots feature the DEGs that were most (A) upregulated and (B) downregulated in old vervets. Venn diagrams show regional overlap in all DEGs that were (C) upregulated and (D) downregulated in old vervets. Each cell lists the number of DEGs as well as the percentage of all DEGs represented by that cell. Venn diagrams were made using Venny 2.1.0.⁵⁷

combined data sets (all four brain regions) and those identified through independent analysis of each region. We first investigated canonical pathways, retaining the “top five” pathways with the greatest negative log uncorrected p -values. Causal network analyses were then implemented to identify gene-dependent regulatory networks associated with DEGs in each brain region, pinpointing “master regulators” affecting notable DEG sub sets. IPA classifies various molecules as regulators, including genes, microRNAs (miRNAs), hormones, and exogenous chemicals. We retained endogenous regulators and disregarded all exogenous chemicals, drugs, and reagents from our regulatory network analyses. To determine whether master regulators were likely activated or inhibited, we used activation Z-score (i.e., an indicator of whether a given regulator is upregulated or downregulated) thresholds of >2 (activated) and <-2 (inhibited).

2.6 | Inferential statistical analyses

For each of the DEGs identified in the analysis of age-related differential expression in the combined data sets, we analyzed expression

levels as a function of $A\beta$ plaque counts, $A\beta_{42}:A\beta_{40}$ ratios, and NE. We used the “corr.test” function in R to generate a series of Pearson’s correlations, running separate correlations for each AD biomarker in the combined data set as well as within individual regions. Thus, for each DEG, we performed 12 correlations (i.e., three AD biomarkers \times expression levels in four brain regions). Correlations were considered “significant” when two-sided uncorrected p -values were <0.05 .

3 | RESULTS

3.1 | Effects of age on gene expression in the combined datasets

Analysis of the combined data sets across the four brain regions yielded 77 DEGs, 51 of which (66%) were upregulated in older vervets. The five genes most upregulated in older individuals across all four brain regions (Figure 1A) were mitochondrial ribosomal protein L17 (MRPL17), late endosomal/lysosomal adaptor, MAPK and MTOR activator 3 (LAMTOR3), estrogen receptor binding site associated antigen

TABLE 1 Differentially expressed genes (DEGs) with the largest fold-changes by age, identified in combined analysis of four brain regions

Direction	Gene symbol	Name	FC	T	p	q (FDR)	B
Upregulated	<i>MRPL17</i>	Mitochondrial Ribosomal Protein L17	2.864	4.562	<0.001	0.023	1.996
	<i>LAMTOR3</i>	Late Endosomal/Lysosomal Adaptor, MAPK And MTOR Activator 3	1.740	6.414	<0.001	0.001	7.344
	<i>EBAG9</i>	Estrogen Receptor Binding Site Associated Antigen 9	1.726	5.653	<0.001	0.003	5.132
	<i>REG1A</i>	Regenerating Family Member 1 Alpha	1.589	4.396	<0.001	0.034	1.533
	<i>LHFPL6</i>	LHFPL Tetraspan Subfamily Member 6	1.476	4.659	<0.001	0.019	2.271
Downregulated	<i>RNU4-1</i>	RNA, U4 Small Nuclear 1	-1.911	-5.425	<0.001	0.004	4.470
	<i>COMMD10</i>	COMM Domain Containing 10	-1.653	-5.057	<0.001	0.008	3.406
	<i>TRO</i>	Trophinin	-1.644	-5.204	<0.001	0.006	3.831
	<i>H4C8</i>	H4 Clustered Histone 8	-1.627	-4.474	<0.001	0.028	1.750
	<i>TYW1B</i>	TRNA-YW Synthesizing Protein 1 Homolog B	-1.586	-5.689	<0.001	0.003	5.238

Abbreviations: B, log-odds of differential expression; FC, fold-change; t, moderated t statistic.

9 (*EBAG9*), regenerating family member 1 alpha (*REG1A*), and LHFPL tetraspan subfamily member 6 (*LHFPL6*). The five most downregulated genes were RNA, U4 small nuclear 1 (*RNU4-1*), COMM domain containing 10 (*COMMD10*), trophinin (*TRO*), H4 clustered histone 8 (*H4C8*), and TRNA-YW synthesizing protein 1 homolog B (*TYW1B*). Cathepsin B (*CTSB*) and *LAMTOR3* exhibited the lowest FDR of any DEGs (8×10^{-4}). Fold changes, *p*-values, and *q*-values/FDR for the five most upregulated and downregulated genes are displayed in Table 1; the full DEG list is available in Table S1.

IPA's canonical pathway analysis indicated five significant pathways associated with the 77 DEGs: (1) hypoxia signaling in the cardiovascular system, (2) *BAG2* signaling pathway, (3) acute phase response signaling, (4) DNA methylation and transcriptional repression signaling, and (5) S-methyl-5'-thioadenosine degradation II. DEGs associated with each pathway are listed in Table 2.

Causal network analysis of the 77 DEGs identified five master regulators with significant directional effects (*Z*-scores > |2|). Three master regulators were inhibited: cyclin C, protease BRCA1 associated protein 1, and polo like kinase 1. The remaining two regulators were activated: kinase group calcium/calmodulin-dependent kinases II and IV and microRNA *miR-29b-3p*. Causal networks, including master regulators, intermediary regulators, and associated DEGs, are displayed in Table 3.

3.2 | Effects of age on gene expression in individual brain regions

Independent DGE analyses for each brain regions yielded 743 DEGs for OB, 759 for PC, 623 for WM, and 136 for ITC. The five most upregulated and downregulated genes in old individuals for each region are displayed in Table 4; full DEG lists for OB, PC, WM, and ITC are available in Tables S2, S3, S4, and S5, respectively. In independent DGE analyses, only two genes were differentially expressed by age across all

four regions: *RNU4-1* and *TRO*, both of which were downregulated in old vervets in all four regions. An additional 25 DEGs were shared by OB, PC, and WM, and are listed in Table S6. Venn diagrams illustrating overlap in regional DEG lists are shown in Figure 1C and D.

The top canonical pathways associated with each brain region were: **OB**, *BEX2* signaling pathway; **PC**, heparan sulfate biosynthesis; **WM**, *PI3K/AKT* signaling; and **ITC**, superpathway of serine and glycine biosynthesis I. The top five canonical pathways for each brain region and associated DEGs are listed in Table 2.

For OB, PC, and WM, we identified 27, 26, and 26 master regulators, respectively, that were either activated or inhibited. DEGs derived from ITC did not yield any significant regulators or causal networks. The master regulators with the highest positive *Z*-scores (i.e., most likely activated) for OB, PC, and WM were the rearranged during transfection (RET) kinase, estrogen receptor alpha (*ESR1*), and tumor protein D52 (*TPD52*), respectively. Master regulators with the most negative *Z*-scores (i.e., most likely inhibited) for OB, PC, and WM were FK506 binding protein (*FKBP5*), mitogen-activated protein kinase kinase 4 (*MAP2K4*), and ubiquitin C-terminal hydrolase L1 (*UCHL1*), respectively. Full lists of master regulators and associated DEGs from each brain region are listed in Table S7.

3.3 | Associations of selected DEGs with AD-associated phenotypes

We previously reported that $A\beta$ plaque counts per unit area as well as extracted $A\beta_{42}$, $A\beta_{40}$, and NE levels were all elevated in the old compared to the middle-aged vervets.²⁰ $A\beta$ plaque counts were significantly positively correlated with age ($\rho = 0.74$, $p = 0.01$), as were $A\beta_{40}$ ($\rho = 0.92$; $p < 0.001$), $A\beta_{42}$ ($\rho = 0.68$; $p = 0.03$), and NE ($\rho = 0.72$, $p = 0.02$) values measured by ELISA. In the current study, the 77 DEGs identified in the combined analyses were used to assess brain region-specific relationships between gene expression and other

TABLE 2 Canonical biological pathways associated with each brain region

Brain region	Ingenuity canonical pathways	–log (p-value)	Ratio	Molecules
Pooled (All Four)	Hypoxia Signaling in the Cardiovascular System	2.90	0.04	CSNK1D, NFKBIB, UBE2M
	BAG2 Signaling Pathway	2.79	0.04	CTSB, PSMC1, PSMF1
	Acute Phase Response Signaling	2.72	0.02	ALB, C1S, NFKBIB, VWF
	DNA Methylation and Transcriptional Repression Signaling	2.37	0.06	H4C3, H4C8
	S-methyl-5'-thioadenosine Degradation II	2.24	0.50	MTAP
OB	BEX2 Signaling Pathway	2.51	0.10	BAD, CCND1, CDKN1A, PGF, PPP2R1B, PPP2R3B, PTEN, SPP1
	3-phosphoinositide Biosynthesis	2.44	0.07	ATP1A2, NUDT12, NUDT9, PIP4K2B, PIP5K1B, PPM1H, PPP1R12B, PPP1R14A, PPP2R1B, PPP2R3B, PTEN, PTPN13, SOCS3, TNS3
	Melanoma Signaling	2.39	0.12	BAD, CCND1, CDKN1A, MRAS, PTEN, RASD2
	Glutathione Redox Reactions II	2.27	0.50	GLRX, GSR
	Ferroptosis Signaling Pathway	2.24	0.08	ABCA1, ALOX12, ALOX15, CDKN1A, CTSB, GLS2, MRAS, NFE2L2, RASD2, SLC1A5
PC	Heparan Sulfate Biosynthesis (Late Stages)	3.33	0.14	CHST7, EXT1, EXTL1, HS3ST2, HS3ST5, HS6ST1, RPE65, SULT4A1
	Heparan Sulfate Biosynthesis	3.00	0.12	CHST7, EXT1, EXTL1, HS3ST2, HS3ST5, HS6ST1, RPE65, SULT4A1
	Pregnenolone Biosynthesis	2.79	0.24	CYP26A1, CYP27A1, CYP4X1, MICAL2
	Proline Biosynthesis I	2.25	0.50	ALDH18A1, PYCR1
	Dermatan Sulfate Biosynthesis (Late Stages)	2.02	0.12	CHST7, HS3ST2, HS3ST5, HS6ST1, SULT4A1
WM	PI3K/AKT Signaling	3.77	0.08	BAD, EIF4E, HSP90AA1, IL17RD, IL27RA, MCL1, NFKBIB, OCRL, PIK3R1, PPP2R2C, PPP2R5D, PTEN, PTGS2, RAP2B, RHEB
	Acute Myeloid Leukemia Signaling	2.68	0.09	BAD, CSF2RA, IDH1, LEF1, MAP2K3, PIK3R1, PML, RAP2B
	Prostate Cancer Signaling	2.67	0.08	BAD, CCNE1, CREB1, HSP90AA1, LEF1, NFKBIB, PIK3R1, PTEN, RAP2B
	Adipogenesis Pathway	2.66	0.08	ATG7, BMPR1B, DDIT3, EGR2, FZD1, KAT7, NR2F2, PER2, RPS6KC1, XBP1
	Circadian Rhythm Signaling	2.49	0.06	CACNA2D4, CACNG6, CIRBP, CREB1, CRY1, CSNK1D, EIF4E, GNG11, GRIN2C, MAP2K3, PER2, PLCD4, PRKAR1A, RAP2B, SOX15
ITC	Superpathway of Serine and Glycine Biosynthesis I	2.32	0.11	NAD, SHMT1
	Integrin Signaling	2.26	0.02	ARF1, ARF3, CDC42, MPRIP, PARVB
	Folate Transformations I	2.00	0.07	NAD, SHMT1
	Colanic Acid Building Blocks Biosynthesis	1.79	0.06	NAD, UGP2
	Ethanol Degradation II	1.76	0.05	ADHFE1, NAD

Note: Pathways were identified using Ingenuity Pathway Analysis.

phenotypes associated with AD neuropathology (P/T cortex AB plaque number, ITC A β 42 and A β 40, and norepinephrine levels). *CTSB* exhibited significant positive relationships with AD biomarkers in 9 of 12 tests (Figure 2). Vacuolar protein sorting 4 homolog A (*VPS4A*), which was negatively correlated with AD biomarkers, exhibited the second highest number of significant correlations (7 of 12 correlations), followed by DNA polymerase delta interacting protein 3 (*POLDIP3*, 5

of 12 positive correlations significant) and *TYW1B* (5 of 12 negative correlations significant). An additional six DEGs (7.8%) exhibited four significant correlations with AD biomarkers, whereas 34 DEGs (44.2%) exhibited three or fewer total significant correlations, and 33 of the 77 DEGs (42.9%) from the combined analysis were not significantly correlated with any of the AD biomarkers in any of the four brain regions. Full lists of significant correlations for A β plaque counts, A β 42:A β 40

TABLE 3 Causal networks associated with combined data set

Master regulator	Name	Molecule type	Participating regulators	Predicted activation	Activation Z-score	P-value	Target molecules in dataset
CCNC	Cyclin C	other	CCNC, CDK19, E2F1	Inhibited	-2.236	0.010	CGRRF1, CTSB, HCG18, NFKBIB, OSGIN1
BAP1	BRCA1 Associated Protein 1	peptidase	BAP1, E2F1, EIF2A, Gamma tubulin, ITPR3, PPARG, PRKAA	Inhibited	-2.236	0.019	ANGPTL4, CTSB, FKBP5, HCG18, NFKBIB
PLK1	Polo Like Kinase 1	kinase	26s Proteasome, Akt, ESR1, MYC, NFKBIA, PLK1, SNCA, TP53, TP63	Inhibited	-2.138	0.008	ALB, CSNK1D, CTSB, FKBP5, FXYD6, GGA2, H4C3, METAP1, NFKBIB, OSGIN1, POLDIP3, REXO4, SETD5, TAX1BP1
miR-29b-3p (and other miRNAs w/seed AGCACCA)		mature microRNA	ERBB2, ERBB3, GATA4, HIF1A, MAPK1, miR-29b-3p (and other miRNAs w/seed AGCACCA), MYC, NFkB (complex), PIK3R1, POU2F2, SP1, STAT1, STAT3, TP53, TP63	Activated	2.183	0.005	ANGPTL4, C1S, CIRBP, CSNK1D, CTSB, FABP5, GGA2, H4C3, LHFPL6, METAP1, METTL23, NUP188, OSGIN1, POLDIP3, REXO4, SIK1/SIK1B, VWF
CaMK-II/IV	Calcium/Calmodulin-Dependent Kinases II and IV	group	CaMK-II/IV, CAMK2A, CAMK2D, CAMK2G, CAMK4, Creb, CREB1, CREM, myosin-light-chain kinase, NFkB (complex), NFKBIA, RARA, RELA, RHOA, STAT3	Activated	2.828	0.017	ANGPTL4, CTSB, FABP5, H4C3, NFKBIB, SETD5, SIK1/SIK1B, THOP1

Note: Networks were identified using Ingenuity Pathway Analysis.

ratios, and NE are available in Tables S8, S9, and S10, respectively. AD biomarker values for each vervet are available in Table S11.

4 | DISCUSSION

Transcriptional profiles obtained from brain regions involved in the olfactory pathway were distinct from one another and were significantly altered by age. Analyses of age effects by region showed two transcripts that were reduced with age across all four brain regions: trophinin (*TRO*) and RNA, U4 small nuclear 1 (*RNU4-1*). *TRO* is expressed in adult mouse brain and appears to play a role in neurogenesis.²⁸ *RNU4-1* is a small nuclear RNA important in brain development²⁹ and is involved with the spliceosome.

In analyses of the combined expression data across brain regions, one of the genes exhibiting the largest upregulation in older vervets was mitochondrial ribosomal protein L17 (*MRPL17*), a critical component of the mitochondrial ribosomal complex. Mitochondrial changes are associated with aging as well as early AD. Late endosomal/lysosomal adaptor, MAPK and MTOR activator 3 (*LAMTOR3*), a gene involved in ERK signaling and the mTOR1 pathway, was also elevated with age, as was FKBP prolyl isomerase 5 (*FKBP5*), which in humans is upregulated with age and associated with a proinflammatory immune profile.³⁰ Genes with large fold-change reductions with age included COMM domain containing 10 (*COMM10*), which

inhibits nuclear factor kappa B (NF- κ B),³¹ a central transcription factor controlling inflammatory gene expression, and TRNA-YW synthesizing protein 1 homolog B (*TYW1B*), which is involved in wybutosine synthesis and has been associated with PHF tau by genome-wide association study (GWAS).³²

Despite these similarities across brain regions, independent analyses pinpointed region-specific patterns of pathway enrichment and regulatory networks. Notably, OB showed a bias toward *BEX2* signaling, which regulates mitochondrial apoptosis,³³ whereas DEGs identified in PC were associated with heparan sulfate biosynthesis; WM, with PI3K/Akt signaling; and ITC, with serine and glycine biosynthesis as well as integrin signaling. It is important to note that all of these pathways have well-supported links to AD and other neurodegenerative diseases. For instance, age-related changes in heparan sulfate proteoglycans and glycosaminoglycans play key roles in the deposition and accumulation of A β plaques,³⁴ and A β may, in turn, stimulate integrin-regulated cell death.³⁵ Glycolysis-derived l-serine impairment in astrocytes drives AD-related cognitive dysfunction in mice,³⁶ whereas AD is associated with generally decreased activity of the PI3K/Akt pathway.³⁷ Exploring region-specific associations with enriched pathways may further explicate mechanisms underlying AD pathogenesis.

Several biological functions unite the DEGs and regulatory networks identified by our analyses. First, several DEGs, pathways, and regulators have known or hypothesized associations with cell death

TABLE 4 Differentially expressed genes (DEGs) with the largest fold changes in individual analysis of each brain region

Brain region	Direction	Gene symbol	Name	FC	t	p	q (FDR)	B
OB	Upregulated	<i>UBD</i>	Ubiquitin D	3.363	4.851	0.000	0.551	-1.533
		<i>MRPL17</i>	Mitochondrial Ribosomal Protein L17	3.259	2.748	0.015	0.848	-3.307
		<i>TAX1BP1</i>	Tax1 Binding Protein 1	2.814	3.448	0.003	0.840	-2.664
		<i>TMA7</i>	Translation Machinery Associated 7 Homolog	2.099	2.339	0.033	0.855	-3.686
		<i>NAPEPLD</i>	N-Acyl Phosphatidylethanolamine Phospholipase D	1.861	2.754	0.015	0.848	-3.301
	Downregulated	<i>PKIA</i>	CAMP-Dependent Protein Kinase Inhibitor Alpha	-2.066	-2.405	0.029	0.855	-3.625
		<i>COMMD10</i>	COMM Domain Containing 10	-1.890	-3.963	0.001	0.807	-2.219
		<i>SPTLC1</i>	Serine Palmitoyltransferase Long Chain Base Subunit 1	-1.817	-2.233	0.041	0.864	-3.782
		<i>RNU4-1</i>	RNA, U4 Small Nuclear 1	-1.758	-2.521	0.023	0.855	-3.518
		<i>COL1A2</i>	Collagen Type I Alpha 2 Chain	-1.709	-2.977	0.009	0.840	-3.094
PC	Upregulated	<i>MRPL17</i>	Mitochondrial Ribosomal Protein L17	2.498	2.171	0.048	0.762	-3.719
		<i>LAMTOR3</i>	Late Endosomal/Lysosomal Adaptor, MAPK And MTOR Activator 3	2.296	5.301	0.000	0.388	-0.023
		<i>CNDP1</i>	Carnosine Dipeptidase 1	2.082	3.560	0.003	0.633	-1.954
		<i>TMA7</i>	Translation Machinery Associated 7 Homolog	2.023	2.630	0.020	0.703	-3.141
		<i>ACTA2</i>	Actin Alpha 2, Smooth Muscle	1.831	2.259	0.041	0.745	-3.610
	Downregulated	<i>MAP1S</i>	Microtubule Associated Protein 1S	-2.193	-3.813	0.002	0.633	-1.643
		<i>DBNDD1</i>	Dysbindin Domain Containing 1	-2.106	-3.185	0.007	0.640	-2.427
		<i>TRO</i>	Trophinin	-1.906	-4.244	0.001	0.604	-1.135
		<i>VPS4A</i>	Vacuolar Protein Sorting 4 Homolog A	-1.823	-5.601	0.000	0.388	0.257
		<i>RNU4-1</i>	RNA, U4 Small Nuclear 1	-1.766	-2.664	0.019	0.703	-3.098
WM	Upregulated	<i>MRPL17</i>	Mitochondrial Ribosomal Protein L17	3.294	2.287	0.041	0.998	-4.142
		<i>TAX1BP1</i>	Tax1 Binding Protein 1	3.047	3.686	0.003	0.998	-3.616
		<i>REG1A</i>	Regenerating Family Member 1 Alpha	2.877	3.395	0.005	0.998	-3.714
		<i>SERPINA3</i>	Serpin Family A Member 3	2.137	2.517	0.027	0.998	-4.049
		<i>EBAG9</i>	Estrogen Receptor Binding Site Associated Antigen 9	1.982	2.797	0.016	0.998	-3.937
	Downregulated	<i>MSRB2</i>	Methionine Sulfoxide Reductase B2	-3.725	-2.679	0.020	0.998	-3.984
		<i>SNORD13</i>	Small Nucleolar RNA, C/D Box 13	-3.079	-2.519	0.026	0.998	-4.048
		<i>RNU4-1</i>	RNA, U4 Small Nuclear 1	-2.648	-3.954	0.002	0.998	-3.531
		<i>DBNDD1</i>	Dysbindin Domain Containing 1	-2.274	-2.356	0.036	0.998	-4.114
		<i>H4C8</i>	H4 Clustered Histone 8	-2.143	-2.912	0.013	0.998	-3.892
ITC	Upregulated	<i>PARVB</i>	Parvin Beta	1.462	3.895	0.002	1.000	-2.412
		<i>ISG20</i>	Interferon Stimulated Exonuclease Gene 20	1.387	3.721	0.002	1.000	-2.547
		<i>ARHGEF40</i>	Rho Guanine Nucleotide Exchange Factor 40	1.382	3.464	0.004	1.000	-2.753
		<i>TRIM66</i>	Tripartite Motif Containing 66	1.329	4.724	0.000	1.000	-1.826
		<i>UNC93B1</i>	Unc-93 Homolog B1, TLR Signaling Regulator	1.318	4.455	0.001	1.000	-2.005
	Downregulated	<i>LOC642072</i>	PREDICTED: Similar to HLA class II histocompatibility antigen	-1.324	-3.731	0.002	1.000	-2.539
		<i>ZC4H2</i>	Zinc Finger C4H2-Type Containing	-1.324	-4.802	0.000	1.000	-1.776
		<i>TMEM108</i>	Transmembrane Protein 108	-1.319	-5.170	0.000	1.000	-1.552
		<i>NOC4L</i>	Nucleolar Complex Associated 4 Homolog	-1.319	-2.786	0.015	1.000	-3.328
		<i>PORCN</i>	Porcupine O-Acyltransferase	-1.302	-4.319	0.001	1.000	-2.100

Abbreviations: B, log-odds of differential expression; FC, fold change; t, moderate t statistic.

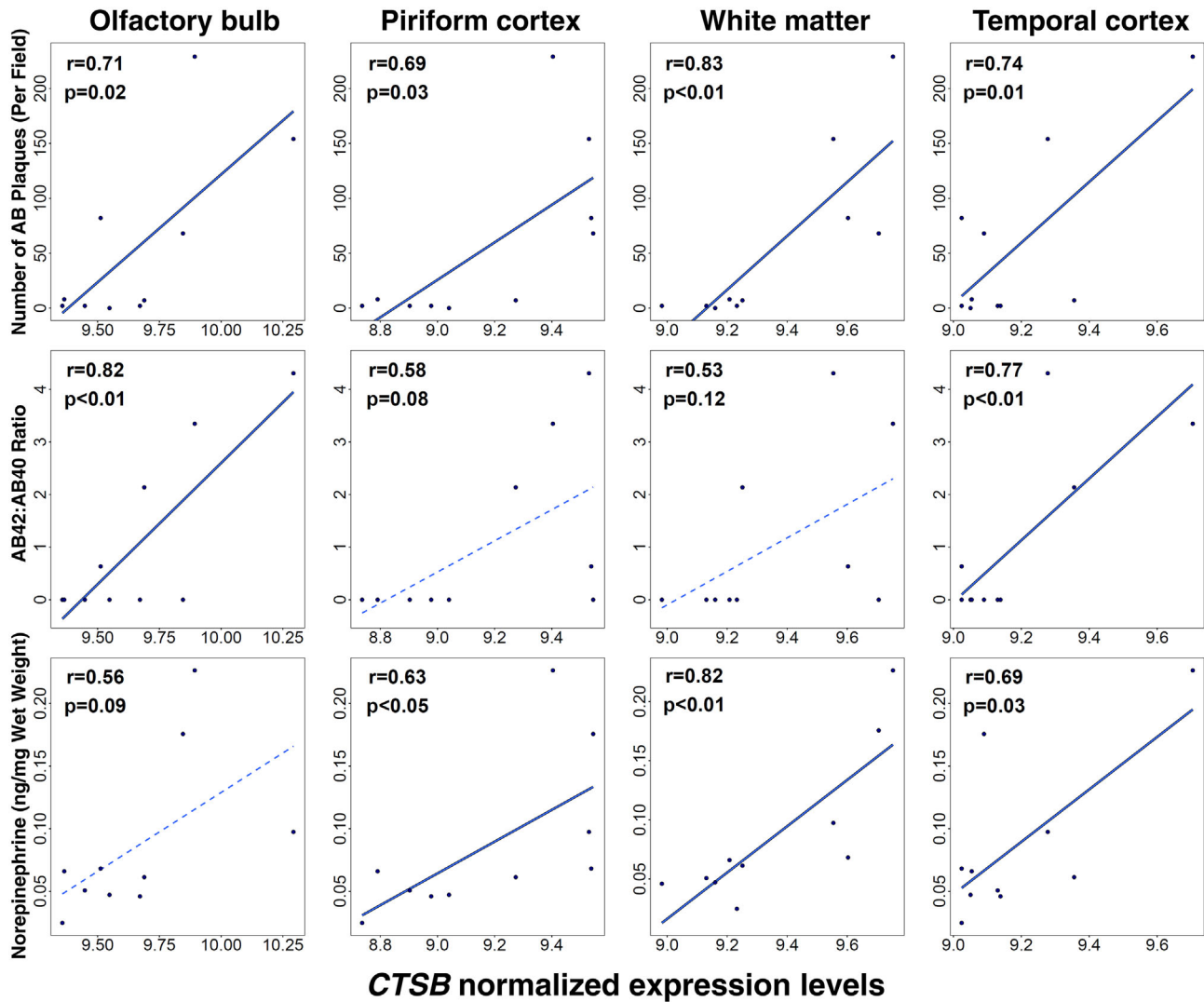


FIGURE 2 Cathepsin B (*CTSB*) expression levels by brain region as predictors of AD biomarkers: A β plaque counts, A β 42:A β 40 ratios, and norepinephrine levels. Solid lines indicate two-sided *p*-values <0.05; dashed lines indicate *p*-values \geq 0.05.

and the inhibition of cell proliferation, including estrogen receptor binding site associated antigen 9 (*EBAG9*), *miR-29b-3p*, NF- κ B, and polo like kinase 1 (*PLK1*).^{38–41} The volume of such targets in our analysis supports the important role of dysregulation of cell death in aging.⁴² Second, regulatory roles were suggested for estrogens and estrogen receptors, given the inclusion of targets such as estrogen receptor 1 (*ESR1*) and *EBAG9*. Finally, these analyses implicate regulatory roles for vascular function. Examples include the differential expression in PC by age of a key regulator of the arterial system—actin alpha 2, smooth muscle (*ACTA2*)⁴³—and the pathway most strongly associated with our cross-regional analysis, which was “hypoxia signaling in cardiovascular system.” Given established links between vascular and brain function, including prominent disorders such as vascular dementia, these data support the important role of vascular impacts on brain aging and neuropathogenesis, and represent a promising area for further investigation.

The genes most strongly correlated with AD biomarkers in our data set have been posited to play a role in AD. Notably, *CTSB*, which

was upregulated in old vervets and most consistently correlated with AD biomarkers, has been linked to AD-related phenotypes in humans and nonhuman animal models. *CTSB* encodes cathepsin B, a lysosomal protease and key regulator of proteosomal homeostasis. Cathepsin B levels increase with age in humans⁴⁴ but are particularly elevated in association with neurocognitive disorders, including AD.⁴⁵ Observed associations between *CTSB* and AD-associated phenotypes likely suggest endolysosomal pathway deficits and collapse of proteostasis. Lysosomal dysfunction is a well-documented component of AD, which contributes to the accumulation of proteins such as A β and tau, which are neuropathological hallmarks of the disease. Consequently, upregulation of *CTSB* in aged vervets with elevated A β plaque counts may represent a compensatory mechanism implemented by lysosomes to reestablish proteostasis, especially given the evidence that cathepsin B reduces A β deposits.⁴⁶ An alternative hypothesis, however, is that cathepsin B plays a causal role in AD development via lysosomal leakage, precipitating cell death, and neuroinflammation.⁴⁵ This hypothesis is supported by evidence from humans and nonhuman models

indicating that cathepsin B inhibition alleviates neurocognitive symptoms of AD.⁴⁵ These differing—although not necessarily incompatible—hypotheses on *CTSB*'s relationship to AD suggest a productive avenue for future research. Finally, given that both *CTSB* and *MRPL17* were upregulated across aged vervet brain regions, and that mitochondrial function may play a role not only in proteostasis generally, but AD-related protein imbalance specifically,⁴⁷ crosstalk between these genetic targets warrants further consideration.

Additional genes for which expression was correlated with AD phenotypes included *VPS4A*, DNA polymerase delta interacting protein 3 (*POLDIP3*), and *TYW1B*. *VPS4A* expression, which was negatively correlated with AD phenotypes, encodes vacuolar protein sorting-associated protein 4A and likely regulates protein trafficking.⁴⁸ In a study of primary skin fibroblasts from 16 mammalian species, *VPS4A* upregulation was observed in longer-lived species.⁴⁹ Critically, in culture, a variant of *VPS4A* causes accumulation of both A β and tau,⁵⁰ suggesting a possible causal role in AD. As for *POLDIP3* and *TYW1B*, both have been identified previously as directly or indirectly associated with neurodegenerative diseases.^{51,52} *POLDIP3* (aka *SKAR*, S6 kinase 1 (S6K1) Aly/REF-like target) mRNA splicing is regulated by transactive response DNA-binding protein-43 (TDP-43),⁵³ an RNA splicing co-factor that contributes to regulation of translation and cell size and has been linked to neurotoxicity, amyotrophic lateral sclerosis, and frontotemporal lobar degeneration.⁵⁴ As noted above, GWASs have shown an association of *TYW1B* with PHF tau.³²

These observations are likely to translate to human health with high fidelity due to the similarity of these NHPs to humans in brain structure, function, patterns of aging, and age-related neuropathology.^{18–21} One limitation of NHPs, including vervets,²¹ is that extensive tauopathy (e.g., neurofibrillary tangles) common to patients with AD is infrequently documented.⁵⁵ Although this difference may constrain direct translation of our results to advanced AD, the model will likely help glean insights into mechanisms that limit tauopathy in NHPs and thus promote the identification of new therapeutic targets. An additional limitation of this study was the relatively small sample size. However, the small sample is mitigated in part by tight experimental controls that eliminate confounding due to diet, housing, diurnal cycles, brain collection while animals were healthy, short and identical post-mortem intervals, and identical post-mortem handling of tissue. Due to a lack of older male vervets in the colony, our study was limited to female vervets. However, females represent an at-risk population, as women exhibit a higher risk of AD.⁵⁶ The IHC assessment of plaque burden was carried out previously in both temporal as well as parietal regions, although we did not assess gene expression in the parietal region and instead focused on temporal cortex as a region more likely involved in early AD pathologies. Future studies would benefit from region-by-region comparisons of transcriptomic variation and AD pathology, as well as inclusion of cognitive assessments, olfactory testing, and neuroimaging to increase our understanding of the functional inter-relationships between these phenotypes. Despite these limitations, our current observations provide a basis for hypothesis generation for future studies.

Collectively, our results indicate age-related variation in gene expression and related biological pathways in several brain regions associated with the olfactory pathway, and that only a subset of age-related genes are also associated with AD-relevant phenotypes. Consequently, our results highlight genes worthy of future investigation in aging NHP and human brain, and also suggest that the approach used here may distinguish processes associated with normal brain aging from those associated with neurodegenerative diseases (i.e., those predictive of neuropathological biomarkers). It is notable that although definitive conclusions cannot be drawn from the patterns observed here, these observations do provide a basis for hypothesis generation to focus future NHP and clinical investigations, and also highlight the value of the vervet model for the study of early AD-like neuropathology.

ACKNOWLEDGMENTS

The authors thank Shannon Macauley and Sarah Kaye for helpful comments on this work. This work was supported by grants from the Department of Pathology of Wake Forest School of Medicine (Thomas C. Register), the National Institutes of Health: RF1AG058829 (Carol A. Shively & Suzanne Craft), R24AG073199 (Shively), Wake Forest Alzheimer's Disease Research Center (P30 AG049638, Suzanne Craft), Vervet Research Colony (P40OD010965, Matthew J. Jorgensen); Claude D. Pepper Older Americans Independence Center of Wake Forest School of Medicine (P30-AG021332); the Roena Kulynych Center for Memory and Cognition Research of Wake Forest School of Medicine; and the Department of Veterans Affairs (Merit Grant, Research Career Scientist Award, VA 247-P-0447, VA 240-12-C-0051).

CONFLICT OF INTEREST

The authors declare no conflicts of interest. Author disclosures are available in the [supporting information](#).

REFERENCES

1. Son G, Jahanshahi A, Yoo S-J, et al. Olfactory neuropathology in Alzheimer's disease: a sign of ongoing neurodegeneration. *BMB Rep*. 2021;54(6):295-304. doi: [10.5483/BMBRep.2021.54.6.055](#)
2. Murphy C. Olfactory and other sensory impairments in Alzheimer disease. *Nature Rev Neurol*. 2019;15(1):11-24. doi: [10.1038/s41582-018-0097-5](#)
3. Duff K, McCaffrey RJ, Solomon GS. The pocket smell test. *J Neuropsychiatry Clin Neurosci*. 2002;14(2):197-201. doi: [10.1176/jnp.14.2.197](#)
4. Su M-W, Ni J-N, Cao T-Y, Wang S-S, Shi J, Tian J-Z. The correlation between olfactory test and hippocampal volume in Alzheimer's disease and mild cognitive impairment patients: a meta-analysis. *Front Aging Neurosci*. 2021;13:755160. doi: [10.3389/fnagi.2021.755160](#)
5. Tian Q, Bilgel M, Moghekar AR, Ferrucci L, Resnick SM. Olfaction, cognitive impairment, and PET biomarkers in community-dwelling older adults. *J Alzheimers Dis*. 2022;86(3):1275-1285. doi: [10.3233/JAD-210636](#)
6. Christen-Zaech S, Kraftsik R, Pilleuvit O, et al. Early olfactory involvement in Alzheimer's disease. *Can J Neurol Sci*. 2003;30(1):20-25. doi: [10.1017/S0317167100002389](#)
7. Wesson DW, Levy E, Nixon RA, Wilson DA. Olfactory dysfunction correlates with amyloid- β burden in an Alzheimer's disease mouse

- model. *J Neurosci*. 2010;30(2):505-514. doi: [10.1523/jneurosci.4622-09.2010](https://doi.org/10.1523/jneurosci.4622-09.2010)
8. Schubert CR, Carmichael LL, Murphy C, Klein BEK, Klein R, Cruickshanks KJ. Olfaction and the 5-year incidence of cognitive impairment in an epidemiological study of older adults. *J Am Geriatr Soc*. 2008;56(8):1517-1521. doi: [10.1111/j.1532-5415.2008.01826.x](https://doi.org/10.1111/j.1532-5415.2008.01826.x)
 9. Adams DR, Kern DW, Wroblewski KE, McClintock MK, Dale W, Pinto JM. Olfactory dysfunction predicts subsequent dementia in older U.S. adults. *J Am Geriatr Soc*. 2018;66(1):140-144. doi: [10.1111/jgs.15048](https://doi.org/10.1111/jgs.15048)
 10. Wheeler PL, Murphy C. Olfactory measures as predictors of conversion to mild cognitive impairment and Alzheimer's disease. *Brain Sci*. 2021;11(11):1391. doi: [10.3390/brainsci11111391](https://doi.org/10.3390/brainsci11111391)
 11. Wilson RS, Arnold SE, Schneider JA, Boyle PA, Buchman AS, Bennett DA. Olfactory impairment in presymptomatic Alzheimer's disease. *Ann N Y Acad Sci*. 2009;1170(1):730-735. doi: [10.1111/j.1749-6632.2009.04013.x](https://doi.org/10.1111/j.1749-6632.2009.04013.x)
 12. Wilson RS, Arnold SE, Schneider JA, Tang Y, Bennett DA. The relationship between cerebral Alzheimer's disease pathology and odour identification in old age. *J Neurol Neurosurg Psychiatry*. 2007;78(1):30-35. doi: [10.1136/jnnp.2006.099721](https://doi.org/10.1136/jnnp.2006.099721)
 13. Peng KY, Mathews PM, Levy E, Wilson DA. Apolipoprotein E4 causes early olfactory network abnormalities and short-term olfactory memory impairments. *Neuroscience*. 2017;343:364-371. doi: [10.1016/j.neuroscience.2016.12.004](https://doi.org/10.1016/j.neuroscience.2016.12.004)
 14. Gilbert PE, Murphy C. The effect of the ApoE ϵ 4 allele on recognition memory for olfactory and visual stimuli in patients with pathologically confirmed Alzheimer's disease, probable Alzheimer's disease, and healthy elderly controls. *J Clin Exp Neuropsychol*. 2004;26(6):779-794. doi: [10.1080/13803390490509439](https://doi.org/10.1080/13803390490509439)
 15. Murphy C, Bacon AW, Bondi MW, Salmon DP. Apolipoprotein E status is associated with odor identification deficits in nondemented older persons. *Ann N Y Acad Sci*. 1998;855(1):744-750. doi: [10.1111/j.1749-6632.1998.tb10654.x](https://doi.org/10.1111/j.1749-6632.1998.tb10654.x)
 16. Linster C, Midroit M, Forest J, et al. Noradrenergic activity in the olfactory bulb is a key element for the stability of olfactory memory. *J Neurosci*. 2020;40(48):9260-9271. doi: [10.1523/JNEUROSCI.1769-20.2020](https://doi.org/10.1523/JNEUROSCI.1769-20.2020)
 17. Gannon M, Che P, Chen Y, Jiao K, Roberson ED, Wang Q. Noradrenergic dysfunction in Alzheimer's disease. Review. *Front Neurosci*. 2015;9:220. doi: [10.3389/fnins.2015.00220](https://doi.org/10.3389/fnins.2015.00220)
 18. Frye BM, Craft S, Latimer CS, et al. Aging-related Alzheimer's disease-like neuropathology and functional decline in captive vervet monkeys (*Chlorocebus aethiops sabaues*). *Am J Primatol*. 2021;83(11):e23260. doi: [10.1002/ajp.23260](https://doi.org/10.1002/ajp.23260)
 19. Frye BM, Valure PM, Craft S, et al. Temporal emergence of age-associated changes in cognitive and physical function in vervets (*Chlorocebus aethiops sabaues*). *Geroscience*. 2021;43(3):1303-1315. doi: [10.1007/s11357-021-00338-w](https://doi.org/10.1007/s11357-021-00338-w)
 20. Kalinin S, Willard SL, Shively CA, et al. Development of amyloid burden in African Green monkeys. *Neurobiol Aging*. 2013;34(10):2361-2369. doi: [10.1016/j.neurobiolaging.2013.03.023](https://doi.org/10.1016/j.neurobiolaging.2013.03.023)
 21. Latimer CS, Shively CA, Keene CD, et al. A nonhuman primate model of early Alzheimer's disease pathologic change: Implications for disease pathogenesis. *Alzheimers Dement*. 2019;15(1):93-105. doi: [10.1016/j.jalz.2018.06.3057](https://doi.org/10.1016/j.jalz.2018.06.3057)
 22. Lemere CA, Beierschmitt A, Iglesias M, et al. Alzheimer's disease AB vaccine reduces central nervous system AB levels in a non-human primate, the Caribbean vervet. *Am J Pathol*. 2004;165(1):283-297. doi: [10.1016/S0002-9440\(10\)63296-8](https://doi.org/10.1016/S0002-9440(10)63296-8)
 23. Atkins HM, Willson CJ, Silverstein M, et al. Characterization of ovarian aging and reproductive senescence in vervet monkeys (*Chlorocebus aethiops sabaues*). *Comp Med*. 2014;64(1):55-62.
 24. Chen JA, Fears SC, Jasinska AJ, et al. Neurodegenerative disease biomarkers A β 1-40, A β 1-42, tau, and p-tau181 in the vervet monkey cerebrospinal fluid: relation to normal aging, genetic influences, and cerebral amyloid angiopathy. *Brain Behav*. 2018;8(2):e00903. doi: [10.1002/brb3.903](https://doi.org/10.1002/brb3.903)
 25. Jasinska AJ, Haghani A, Zoller JA, et al. Epigenetic clock and methylation studies in vervet monkeys. *Geroscience*. 2022;44(2):699-717. doi: [10.1007/s11357-021-00466-3](https://doi.org/10.1007/s11357-021-00466-3)
 26. Ritchie ME, Phipson B, Wu D, et al. *limma* powers differential expression analyses for RNA-sequencing and microarray studies. *Nucleic Acids Res*. 2015;43(7):e47. doi: [10.1093/nar/gkv007](https://doi.org/10.1093/nar/gkv007)
 27. R: A language and environment for statistical computing. R Foundation for Statistical Computing; 2021. <https://www.R-project.org>
 28. Ma L, Yin M, Wu X, et al. Expression of trophinin and bystin identifies distinct cell types in the germinal zones of adult rat brain. *Eur J Neurosci*. 2006;23(9):2265-2276. doi: [10.1111/j.1460-9568.2006.04782.x](https://doi.org/10.1111/j.1460-9568.2006.04782.x)
 29. Ederly P, Marcaillou C, Sahbatou M, et al. Association of TALS developmental disorder with defect in minor splicing component *U4atac* snRNA. *Science*. 2011;332(6026):240-243. doi: [10.1126/science.1202205](https://doi.org/10.1126/science.1202205)
 30. Zannas Anthony S, Jia M, Hafner K, et al. Epigenetic upregulation of FKBP5 by aging and stress contributes to NF- κ B - driven inflammation and cardiovascular risk. *Proc Natl Acad Sci USA*. 2019;116(23):11370-11379. doi: [10.1073/pnas.1816847116](https://doi.org/10.1073/pnas.1816847116)
 31. Ganesh L, Burstein E, Guha-Niyogi A, et al. The gene product Murr1 restricts HIV-1 replication in resting CD4+ lymphocytes. *Nature*. 2003;426(6968):853-857. doi: [10.1038/nature02171](https://doi.org/10.1038/nature02171)
 32. Wang H, Yang J, Schneider JA, De Jager PL, Bennett DA, Zhang H-Y. Genome-wide interaction analysis of pathological hallmarks in Alzheimer's disease. *Neurobiol Aging*. 2020;93:61-68. doi: [10.1016/j.neurobiolaging.2020.04.025](https://doi.org/10.1016/j.neurobiolaging.2020.04.025)
 33. Naderi A, Liu J, Bennett IC. BEX2 regulates mitochondrial apoptosis and G1 cell cycle in breast cancer. *Int J Cancer*. 2010;126(7):1596-1610. doi: [10.1002/ijc.24866](https://doi.org/10.1002/ijc.24866)
 34. Snow AD, Cummings JA, Lake T. The unifying hypothesis of Alzheimer's disease: heparan sulfate proteoglycans/glycosaminoglycans are key as first hypothesized over 30 years ago. Review. *Front Aging Neurosci*. 2021;13:710683. doi: [10.3389/fnagi.2021.710683](https://doi.org/10.3389/fnagi.2021.710683)
 35. Caltagarone J, Jing Z, Bowser R. Focal adhesions regulate A β signaling and cell death in Alzheimer's disease. *Biochim Biophys Acta*. 2007;1772(4):438-445. doi: [10.1016/j.bbadis.2006.11.007](https://doi.org/10.1016/j.bbadis.2006.11.007)
 36. Le Douce J, Maugard M, Veran J, et al. Impairment of glycolysis-derived L-serine production in astrocytes contributes to cognitive deficits in Alzheimer's disease. *Cell Metab*. 2020;31(3):503-517.e8. doi: [10.1016/j.cmet.2020.02.004](https://doi.org/10.1016/j.cmet.2020.02.004)
 37. Gabbouj S, Ryhänen S, Marttinen M, et al. Altered insulin signaling in Alzheimer's disease brain - special emphasis on PI3K-Akt pathway. *Front Neurosci*. 2019;13:629. doi: [10.3389/fnins.2019.00629](https://doi.org/10.3389/fnins.2019.00629)
 38. Chen L, Li Q, Wang J, et al. MiR-29b-3p promotes chondrocyte apoptosis and facilitates the occurrence and development of osteoarthritis by targeting PGRN. *J Cell Mol Med*. 2017;21(12):3347-3359. doi: [10.1111/jcmm.13237](https://doi.org/10.1111/jcmm.13237)
 39. Nakashima M, Sonoda K, Watanabe T. Inhibition of cell growth and induction of apoptotic cell death by the human tumor-associated antigen RCAS1. *Nat Med*. 1999;5(8):938-942. doi: [10.1038/11383](https://doi.org/10.1038/11383)
 40. Khandelwal N, Simpson J, Taylor G, et al. Nucleolar NF- κ B/RelA mediates apoptosis by causing cytoplasmic relocalization of nucleophosmin. *Cell Death Differ*. 2011;18(12):1889-1903. doi: [10.1038/cdd.2011.79](https://doi.org/10.1038/cdd.2011.79)
 41. Liu X, Erikson Raymond L. Polo-like kinase (Plk)1 depletion induces apoptosis in cancer cells. *Proc Natl Acad Sci USA*. 2003;100(10):5789-5794. doi: [10.1073/pnas.1031523100](https://doi.org/10.1073/pnas.1031523100)
 42. Tower J. Programmed cell death in aging. *Ageing Res Rev*. 2015;23:90-100. doi: [10.1016/j.arr.2015.04.002](https://doi.org/10.1016/j.arr.2015.04.002)
 43. Guo D-C, Papke CL, Tran-Fadulu V, et al. Mutations in smooth muscle alpha-actin (ACTA2) cause coronary artery disease, stroke, and moyamoya disease, along with thoracic aortic disease. *Am J Hum Genet*. 2009;84(5):617-627. doi: [10.1016/j.ajhg.2009.04.007](https://doi.org/10.1016/j.ajhg.2009.04.007)

44. Nilsson E, Bodolea C, Gordh T, Larsson A. Cerebrospinal fluid cathepsin B and S. *Neurol Sci*. 2013;34(4):445-448. doi: [10.1007/s10072-012-1022-0](https://doi.org/10.1007/s10072-012-1022-0)
45. Hook V, Yoon M, Mosier C, et al. Cathepsin B in neurodegeneration of Alzheimer's disease, traumatic brain injury, and related brain disorders. *Biochim Biophys Acta Proteins Proteom*. 2020;1868(8):140428. doi: [10.1016/j.bbapap.2020.140428](https://doi.org/10.1016/j.bbapap.2020.140428)
46. Mueller-Steiner S, Zhou Y, Arai H, et al. Anti-amyloidogenic and neuroprotective functions of cathepsin B: implications for Alzheimer's disease. *Neuron*. 2006;51(6):703-714. doi: [10.1016/j.neuron.2006.07.027](https://doi.org/10.1016/j.neuron.2006.07.027)
47. Weidling IW, Swerdlow RH. Mitochondria in Alzheimer's disease and their potential role in Alzheimer's proteostasis. *Exp Neurol*. 2020;330:113321. doi: [10.1016/j.expneurol.2020.113321](https://doi.org/10.1016/j.expneurol.2020.113321)
48. Seu KG, Trump LR, Emberesh S, et al. VPS4A mutations in humans cause syndromic congenital dyserythropoietic anemia due to cytokinesis and trafficking defects. *Am J Hum Genet*. 2020;107(6):1149-1156. doi: [10.1016/j.ajhg.2020.10.013](https://doi.org/10.1016/j.ajhg.2020.10.013)
49. Ma S, Upneja A, Galecki A, et al. Cell culture-based profiling across mammals reveals DNA repair and metabolism as determinants of species longevity. *Elife*. 2016;5:e19130. doi: [10.7554/eLife.19130](https://doi.org/10.7554/eLife.19130)
50. Willén K, Edgar JR, Hasegawa T, Tanaka N, Futter CE, Gouras GK. A β accumulation causes MVB enlargement and is modelled by dominant negative VPS4A. *Mol Neurodegener*. 2017;12(1):61. doi: [10.1186/s13024-017-0203-y](https://doi.org/10.1186/s13024-017-0203-y)
51. George G, Singh S, Lokappa SB, Varkey J. Gene co-expression network analysis for identifying genetic markers in Parkinson's disease – a three-way comparative approach. *Genomics*. 2019;111(4):819-830. doi: [10.1016/j.ygeno.2018.05.005](https://doi.org/10.1016/j.ygeno.2018.05.005)
52. Lu J, Huang R, Peng Y, et al. Effects of DISC1 on Alzheimer's disease cell models assessed by iTRAQ proteomics analysis. *Biosci Rep*. 2022;42(1):BSR20211150. doi: [10.1042/BSR20211150](https://doi.org/10.1042/BSR20211150)
53. Fiesel FC, Weber SS, Supper J, Zell A, Kahle PJ. TDP-43 regulates global translational yield by splicing of exon junction complex component SKAR. *Nucleic Acids Res*. 2012;40(6):2668-2682. doi: [10.1093/nar/gkr1082](https://doi.org/10.1093/nar/gkr1082)
54. Suzuki H, Shibagaki Y, Hattori S, Matsuoka M. Nuclear TDP-43 causes neuronal toxicity by escaping from the inhibitory regulation by hnRNPs. *Hum Mol Genet*. 2015;24(6):1513-1527. doi: [10.1093/hmg/ddu563](https://doi.org/10.1093/hmg/ddu563)
55. Walker LC, Jucker M. The exceptional vulnerability of humans to Alzheimer's disease. *Trends Mol Med*. 2017;23(6):534-545. doi: [10.1016/j.molmed.2017.04.001](https://doi.org/10.1016/j.molmed.2017.04.001)
56. Seshadri S, Wolf PA, Beiser A, et al. Lifetime risk of dementia and Alzheimer's disease. *Neurology*. 1997;49(6):1498. doi: [10.1212/WNL.49.6.1498](https://doi.org/10.1212/WNL.49.6.1498)
57. Oliveros JC, Venny. An interactive tool for comparing lists with Venn's diagrams. 2007-2015. <https://bioinfogp.cnb.csic.es/tools/venny/index.html>

SUPPORTING INFORMATION

Additional supporting information can be found online in the Supporting Information section at the end of this article.

How to cite this article: Negrey JD, Dobbins DL, Howard TD, et al. Transcriptional profiles in olfactory pathway-associated brain regions of African green monkeys: Associations with age and Alzheimer's disease neuropathology. *Alzheimer's Dement*. 2022;8:e12358. <https://doi.org/10.1002/trc2.12358>